Frontiers of Information Technology & Electronic Engineering
www.jzus.zju.edu.cn; engineering.cae.cn; www.springerlink.com
ISSN 2095-9184 (print); ISSN 2095-9230 (online)
E-mail: jzus@zju.edu.cn

A platform of digital brain using crowd power*

Dongrong XU‡[1], Fei DAI[1,2], Yue LU[2]

[1]*Columbia University & New York State Psychiatric Institute, NY 10032, USA*

[2]*Shanghai Key Laboratory of Multidimensional Information Processing, East China Normal University, Shanghai 200062, China*

E-mail: xu.dongrong@columbia.edu; fd2331@columbia.edu; ylu@cs.ecnu.edu.cn

Received Nov. 30, 2017; Revision accepted Jan. 20, 2018; Crosschecked Jan. 22, 2018

Abstract: A powerful platform of digital brain is proposed using crowd wisdom for brain research, based on the computational artificial intelligence model of synthesis reasoning and multi-source analogical generating. The design of the platform aims to make it a comprehensive brain database, a brain phantom generator, a brain knowledge base, and an intelligent assistant for research on neurological and psychiatric diseases and brain development. Using big data, crowd wisdom, and high performance computers may significantly enhance the capability of the platform. Preliminary achievements along this track are reported.

Key words: Artificial intelligence; Digital brain; Synthesis reasoning; Multi-source analogical generating; Crowd wisdom; Deducing; Neuroimaging

https://doi.org/10.1631/FITEE.1700800 **CLC number:** TP391

1 Introduction

Human brain is the most advanced instrument in the world, and has been largely responsible for the development of civilization. An extremely large number of studies on the brain have been conducted, covering multiple aspects and perspectives. The studies include, but are not limited to, those in biology, biochemistry, biophysics, genetics, physiology in the domain of basic sciences, psychology, psychiatry, cognition in social studies and medical research, and those in artificial intelligence, human-brain interfacing in the domains of computer science and bioengineering, aiming to simulate human intelligence using the machine. There have been hundreds of thousands of publications on the brain, with thousands more each year. New findings and knowledge on the brain are being accumulated, becoming progressively more complex, and thereby more difficult to manage and learn.

Compared to the knowledge in other basic sciences, such as mathematics, physics, biology, and chemistry, knowledge on human brains is still very sparse. The mechanism of how brain works largely remains a mystery, as it appears to be a black box to humans. Conventional and traditional approaches typically indirectly study the brain, for example, behavioral studies, which observe the behavior of human brains to infer how brain works, or neurosurgery, which may correlate functions with specific brain regions from patients of traumatic brain injury. Recent advances in science and technology have provided novel means for investigating brain mechanism more directly. Brain imaging, such as functional magnetic resonance imaging (fMRI) (Baars and Gage, 2010; Brown et al., 2014), may directly observe activities in brain regions by detecting blood-oxygen-level dependent (BOLD) signals in tissue by relating the signals to a task that is being performed, while the task can be a cognitive, psychological, or motor one. For example, the hippocampus will show activation

‡ Corresponding author

* Project supported by the National Key R&D Program of China (No. 2017YFC1308502) and the National Natural Science Foundation of China (No. 81471734)

ORCID: Dongrong XU, http://orcid.org/0000-0003-4682-1587

when a person is executing a memory and spatial learning task; the visual cortex is active in fMRI when a person is watching a video, and the M1 motor cortex will light up in fMRI when a person is tapping fingers. Optogenetics now allows the visualization of the transmission of a neuron firing on a scale of milliseconds and the recording of its transmission pathways in the neural system. However, these advances are not adequate to understand and address the most basic question concerning how exactly a human brain works when thinking and how exactly it could have self-cognition.

With the vast existing body of research and continuing development, as mentioned above, no one can know even a small fraction, say 10%, of the work. Thus, there is a significant risk that a researcher will be unaware of relevant past findings such that in some cases, people may unnecessarily repeat work, which is a waste of resources. Therefore, it would be desirable to have a method that can automatically collect, preserve, sort, manage, and use the knowledge of all the brain research. It would be even desirable if new knowledge may be generated based on what is already known.

Synthesis reasoning (SR) (Pan, 1996), also known as multi-source analogical generating (MSAG) (Xu, 1995; Xu and Pan, 1995), is a computational model originally developed for intelligent computer-aided design (iCAD), which aims to simulate the creative power of human designers using computer programs or the machine. Conventional CAD systems are passive tools for implementation of designs or solutions that human beings have already created. For example, Microsoft Word is a powerful editing software tool, but it cannot compose an article for you; Adobe Photoshop is useful in producing nice and beautiful visual effects, but a human artist has to first design the creation. SR and MSAG have provided a way for upgrading a CAD system to be an intelligent helper for human designers, thereby making it an iCAD system. For example, an iCAD system of newspaper page layout (Xu, 1998) may automatically generate a handful of draft solutions as needed for the current list of news and photographs to be published on the same page for today's newspaper. It generates in just one click the solutions that meet specific rules and requirements of the layout of a unique style, based on published cases that are thought to have met the particular requirements. Therefore, human editors may just need to select one or two from them and then slightly adjust the draft layout for finalization, and sign to publish. In this way, it is no longer necessary to manually count the number of characters and plan an area for each news coverage on the same page for all the news coverages to fit nicely onto the same page, which typically takes several hours of manual labor. As another example, following a limited number of requirements regarding factors such as color schema, pattern type, and layout pattern, an iCAD system for carpet or cloth pattern design (Pan, 1997) may also automatically retrieve the respective elements meeting the individual aspects of requirements from an art-material database and generate right away hundreds of new designs for a human designer to refer to. In these instances, the iCAD systems may not ultimately replace a human designer, but they really work as an intelligent assistant, greatly relieving the load of human labor.

Artificial intelligence (AI), initiated in the 1950s, forcefully revived recently after having experienced three 'winters' in 1970s and 1980s, respectively, due to technical difficulties that cannot be overcome. Attributed to the significant development of Internet-related technology and its popular use nowadays, and also the significant improvement of computational power of contemporary computers that has never been achieved, big data management and deep learning are now possible. Therefore, the current wave of AI relies heavily on the use of crowd wisdom (Michelucci and Dickinson, 2016) and the knowledge graph (Nickel et al., 2016), which cannot live without the soil of the Internet and the extremely powerful computers. Google search engine, Google advertisements, Google maps & navigation, Amazon's virtual assistant (Echo/Alexa), IBM Watson, and Apple Siri are typical examples. SR/MSAG, an AI computational model that is capable of employing crowd wisdom and big data, and combining different types of knowledge, is particularly suitable for knowledge computation and production.

In this work, we propose to use SR/MSAG to build a powerful platform of the digital brain using crowd wisdom for brain research. The design of the platform aims to make it a powerful brain database, a brain phantom generator, a brain knowledge base, and an intelligent research and diagnosis assistant for

neurological and psychiatric disease study and brain development. We report the preliminary progress that we have achieved thus far along this track.

2 Method

SR/MSAG is a computational theory originally developed for iCAD. Its computational framework gives computer programs a great degree of creativity (computational intelligence). iCAD systems employ it for automated design of innovative products, simulating what a human designer can do. A synonym for synthesis reasoning (Pan, 1996, 1997), MSAG was developed from analogical reasoning (AR). MSAG works in a way just as a mother and a father that can give birth to new babies. The babies inherit various characteristics from the same set of features from the same parents, and therefore they are alike; however, they are also distinctive individuals, due to their inheritance of different subsets of the features. The resemblance to the parents assures that they are of the same species, whereas the difference from the parents and their siblings guarantees that they are completely new. The theoretical assumption behind MSAG is that any invention is ultimately a discovery—the object being invented actually already exists (however, often intangibly instead of physically), but was not conceptually perceived easily. It was not perceived because it is in a very high dimensional space of features that is usually beyond the direct cognitive ability and imagination of human beings. In this view, new things are not exactly new but simply are not recognized because of lack of cognitive ability. Therefore, inventing new things could be largely equivalent to exploring something based on certain rules in a very high dimensional space that the real world has already constructed for us. This concept basically has pointed the way to how a computer program may possibly possess the power of creativity.

Taking the parents-children example, we know that a father and a mother are potentially able to produce many individual children. While the parents are absolutely two different individuals, each child resembles the parent to a certain degree but is certainly not exactly the same (which founds the property ‘new’); also, the children are alike but different from each other. The children of the same parents are the concrete instances resulting from permuting numerous genes that are paired. The extremely large number of genes coins the feature of variety within the very high dimensional space of genes, and the correspondence of genes (paring) across the parents guarantees that the product is perfectly organized and structured in a consistent way as do the parents. Now consider that the parents are replaced by (more than two) items that are not biological, and that their genes are analogous to various features; thus, the multiple parents form a hyper-field and span a high dimensional feature space, with each dimension representing one particular feature (Xu, 1995; Xu and Pan, 1995). Any point within the hyper-field of this space spanned by these parents is potentially their child, with its distance from a parent defining the resemblance to that particular parent (thinking of the magnetic force that a piece of iron may receive if three or more magnets are distributed in its vicinity, jointly forming a magnetic field). The child will resemble each parent to different degrees in different feature aspects, depending on the parent source of each feature and the associated distance to the parent, with the distance defining the resemblance. To illustrate the idea, if we take human facial sketches as the ‘parents’, we can produce new cartoon characters (Fig. 1), in which the features refer to the shapes and locations of the facial features (Rhodes et al., 1987; Fan, 2013; Fan et al., 2014).

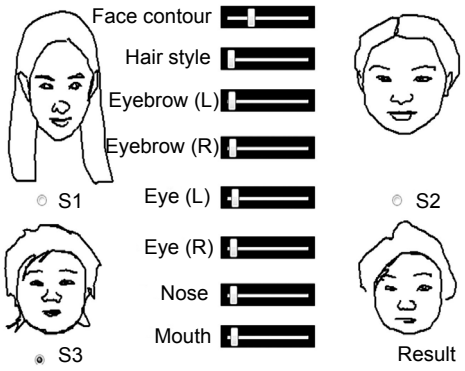

Fig. 1 A multi-source analogical generating (MSAG) application

Three sources S1, S2, and S3 are used and the lower-right is the generated result, which mixes different features with different weights from S1–S3. The scroll bars define the similarity weights to the sources (in the current snapshot, to S3). Notably, this allows the generation of numerous results in the continuous hyper-space spanned by S1, S2, and S3

All human brains are generally similar. For example, each has two hemispheres, and consists of white matter (WM), grey matter (GM), and four brain ventricles, and cortical folding spreads throughout the brain surface and each hemisphere has several lobes with a number of major gyri and sulci. Also, MR T1-relaxation time of newborns is always longer in WM than in GM, and shorter in WM of adults than in GM, without exception. Brain functioning areas generally locate in similar regions in the brain; e.g., the hippocampus is related to spatial learning and memory (Lynch, 1979; Packard and White, 1991; Squire, 1992; Shapiro and Eichenbaum, 1999; Maguire, 2001), Broca's area is responsible for speech and language processing (Amunts et al., 1999; Hagoort, 2005; Baars and Gage, 2010), and the visual cortex locates at the occipital lobe (Belliveau et al., 1991; DeYoe et al., 1996; Bradley et al., 2003). Nevertheless, no two brains are exactly the same, either morphologically, structurally, functionally, biologically, psychologically, or histologically. Even with those subjects acquired on the same MRI scanner using the same acquisition parameters, significant inter-subject variances can be observed in the images (van Hecke et al., 2009). Taking multiple brains as the parents (base brains) in MSAG, and classifying them along different axes of many features (e.g., age, gender, shape, size, structure, voxel intensity, and T1/T2 relaxation times), we can construct a hyper-space of brains. In this space, every point is potentially a new human brain (Fig. 2), which resembles the base brains, but also differs from the base brains in every feature aspect. Therefore, applying MSAG to neuroimaging will allow the production of countless new brain images.

MRI data: We used MR imaging data in this work. We acquired T1-weighted (T1w), T2-weighted (T2w), T1/T2 relaxation, and diffusion-weighted/diffusion tensor imaging (DWI/DTI) data. Although many MRI datasets and databases can be downloaded online (Arnold et al., 2001; Aubert-Broche et al., 2006; Evans, 2006; Jack et al., 2008; Hagmann et al., 2010; Sporns, 2011; Toga et al., 2012; van Essen et al., 2013), such as the National Database for Autism Research (NDAR, www.ndar.nih.gov), the ABCD study (abcdstudy.org), and the BRAINnet database (www.brainnet.net), none of them provides a comprehensive set of all the data modalities that we need in this project. Because combining imaging data of different MR modalities from different sources requires extra work to calibrate the signals, bias control will be hard to justify. Therefore, we acquired five complete sets of highly consistent and good quality imaging data from real subjects to prototype construction of a solid database to build our model.

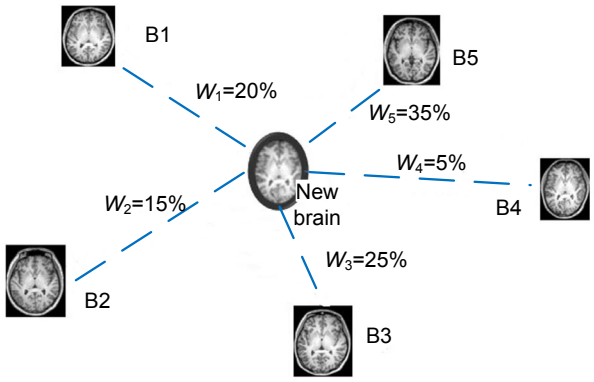

Fig. 2 The proposed platform using MSAG to generate new brains, which currently employs five base brains with scalp

The brains are distributed on a plane, composing a five-source generation field. Any location on this plane is potentially an MSAG result. In the current example, the new brain in the middle has weights of 0.2, 0.15, 0.25, 0.05, and 0.35, representing the similarity of this new brain to the five base brains. The locations of all the five bases and that of the new brain can be freely moved, resulting in different weighting factors and consequently different new brains

Data processing: All images were de-identified to protect privacy as required by HIPPA. The imaging data were visually inspected to exclude those containing obvious artifacts due to motion, thermal, or other artifacts and noise. Next, we quantitatively examined the data using a tool developed in-house to exclude those containing invisible motion or distortion that exceeds 1.5 degrees of rotation or 1 mm of translation (Xu et al., 2003, 2008; Liu W et al., 2012b; Liu X, 2013; Wen et al., 2013). Subsequently, we isolated non-brain tissue for each brain, including scalp, cerebellum, and brain stem. We first used the brain extraction tool (BET) (Fagiolo et al., 2008) provided by the FMRIB Software Library (FSL) to roughly segment the brain. Then a research assistant trained in human brain anatomy performed a careful and detailed manual editing using our 3D image editing tool VolEdit to correct in three orthogonal

views voxel by voxel the residuals and connecting dura that were not successfully removed by BET.

DWI/DTI data require additional preprocessing steps, which correct them for eddy-current induced distortion (Haselgrove and Moore, 1996; Bastin, 1999, 2001; Bastin and Armitage, 2000; Zhuang et al., 2006; Liu W et al., 2012a), so that the raw DWI data acquired along different gradient directions were co-registered with the baseline images. This ensures that corresponding voxels across all the DWI volumes for the same subject are measuring exactly the same tissue location, and further processing of the DWI data such as tensor reconstruction, diffusion anisotropy index (DAI) calculation, and fiber tracking will be accurate.

Knowledge extraction: To make it a qualified base brain, each raw dataset was preprocessed, and necessary knowledge of the brain in every aspect in terms of morphology, intensity, and information about tissue properties and imaging parameters was collected and recorded: (1) We first performed a *K*-means fuzzy segmentation (Kanungo et al., 2002; Ng et al., 2006) on each brain using its T1w data to identify five structural components, i.e., WM, GM, ventricle cerebrospinal fluid (vCSF), cortical CSF (cCSF), and background (BG). Standard smoothing operations were performed to remove noise and small holes in each component to generate reasonable tissue classifications. A brain mask containing five segmented regions was thus defined for each participant brain for future use in this study. (2) We recorded the border of the five components, as well as those of the removed non-brain tissues. (3) We also slightly regulated the voxel intensity so that the value ranges of all the brain voxels were separated into four bins (WM, GM, CSF, and BG), with a delimiter interval (DI) at the boundary of the neighboring value ranges of different tissue components, using an equation similar to that developed in the preliminary work (Bansal et al., 2013): $I_v \times (-\mathrm{DI}(x-A_b)/A_r+W)$, where I_v is the measured voxel intensity, DI a small value defining the delimiter interval, x the current age, A_b=20 the base age for the deducing, A_r the ceiling age for simulation, and W=81% (GM) or 69% (WM) the water content percentage at the base age (Neeb et al., 2006; Bansal et al., 2013). This minor regulation of the voxel intensity range helped prevent tissues in the generated data from being segmented into the wrong categories but will not change the intrinsic relaxation properties. (4) We estimated T1, T2 times for each voxel in each base brain, using the technique described in our preliminary studies (Liu F et al., 2006, 2008, 2010; Bansal et al., 2013). (5) We recorded all demographic information that was collectable, such as age, sex, race, handedness, and educational background as it is known that these variables contribute to brain variability (Hsu et al., 2008; Huster et al., 2009; van Hecke et al., 2009). Such information was useful for defining the ethnicity and background of a brain and its datasets to be prescribed and deduced. Consequently, we had set up for each base brain a very high dimensional space of features, and thus the base brains spanned a very high dimensional space for deducing new brain images. Every point in this hyperspace potentially corresponds to a new brain, defined by all the computable features associated to the base brains that had been constructed thus far. Now, the only remaining piece was the correspondence of the features across the base brains, which decided how the extracted features were to be matched for reasoning (just like pairing allele genes from individual parents), and this is key to reasoning within MSAG for deducing realistic new brain data.

Spatial normalization: To set up the correspondence between all the base brains to match the corresponding features, we spatially normalized all the imaging data to the MNI_152_T1_1mm template. A local transformation D_L normalized all the base brains (after preprocessing) first to their local template within each base brain using a 3D normalization (Davatzikos et al., 2001; Shen and Davatzikos, 2002, 2003; Bansal et al., 2012), followed by another step of 3D spatial normalization (D_G) that maps all the local template brains to the final template (Shen and Davatzikos, 2004; Shen et al., 2005; Schreibmann et al., 2008; Lorenzi et al., 2010; Bansal et al., 2012; Hao et al., 2013). (1) D_L: for each base brain, we selected its high-resolution T1w as the local brain template and normalized all the data of other modalities to this local template using a cross-modality method that maximizes mutual information (Davatzikos, 1996a, 1996b, 1997; Shen and Davatzikos, 2002, 2003; Bansal et al., 2005; van Hecke et al., 2009; Hao et al., 2013). (2) D_G: in this step, we set up spatial correspondence from all the local T1w templates to the final MNI_152_T1_1mm template. Combining D_L

and D_G, we normalized all the MRI data to the template space. Thus, the voxel correspondence between any two brains or two images was defined. After the images were co-registered to the template MNI_152 space which had already been carefully defined with 124 regions (Bohland et al., 2009), the tissue type classification of each voxel in the base brains was defined.

Brain correspondence: With the spatial correspondences set up for every voxel in every base brain in the MSAG reasoning space, knowledge and features across the base brains were properly linked and matched. These matched brains were ready to be used just like the 'allele genes' for generating new brains that would also bear all these features. In particular, it would define in the new brain its WM, GM, CSF, their boundaries, nonbrain tissues, voxel properties, and associated demographic information.

Deducing new brains: New brains were to be generated following the MSAG schema in the space spanned by the base brains. Every aspect of the new brains was generated as a weighted sum of the corresponding aspect of the base brains. Once all the aspects of a new brain were generated, a new brain was defined. Suppose we use N base brains. The i^{th} feature aspect F_i of the new brain can be computed as $F_i=\sum_{k=1,2,\ldots,N} W_i^K F_i^K$, where W_i^K is the weighting factor of the i^{th} feature of the k^{th} base brain, and F_i^K is the corresponding i^{th} feature of the k^{th} base brain. W_i^K is decided by the relative distance of the new brain in the MSAG space from the k^{th} base brain (the closer, the larger), normalized by the sum of distances from the new brain to all the base brains employed for this deduction (Fig. 2).

In this process, several factors can be adjusted to control the MSAG reasoning behavior: (1) The base brains can be selected with criteria, so that particular requirements can be met. For example, select only female base brains to generate a female brain, or select male Caucasian base brains at 30 s to simulate data of such a particular population, or use base brains of young Black and Caucasian participants with a college degree as parents to simulate their hybrid offspring already grown to approximately the same age range. (2) The base brains adopted are distributed at will to form a favorable MSAG field (Fig. 2). Once the distribution is determined, an MSAG field is set up and any point within the field represents a potential MSAG result of a new brain. (3) The closer the location of the new brain to a base brain, the higher the similarity between this new brain and that particular base brain. (4) Different features can use differing weight settings. In other words, the setting in Fig. 2 does not have to apply to all features, but each feature may configure its own version of weighting. (5) The number of base brains can vary, as long as it is more than two. Certainly, the more that enter into the MSAG process, the more versatile the results can be. (6) Brain MRI data of different imaging modalities (T1w, T2w, T1/T2-maps) can be ordered at the determined location, as if an MR scanner scanned the same person's brain for the different MRI modalities. (7) The inclusion of features can be adjusted as needed, and only the selected features will be controlled for deducing results. For example, if only sex and age are of interest, the deduced data will show variances reflecting only sex and age, but with all other features averaged in default demonstrating a statistical pattern as will be shown in a brain atlas. New brains can thus be prescribed as needed.

3 Experiments

To validate the proposed idea and demonstrate its feasibility, we conducted three preliminary experiments.

In the first experiment, we used five healthy adults' brains as the base brains. The five brains differ from each other significantly in morphometry (Fig. 3), i.e., shape, GM/WM distribution, cortex thickness, location and size of major gyri/sulci, and ventricles. By adjusting the relative positions and distance between the expected result and the base brains in the space spanned by the base brains (Fig. 2) for each individual aspect, the model can generate various new brains with new attributes inherited and blended from the base brains, respectively, according to the relative spatial setting in the MSAG space. For example, we can choose to generate a new image that simulates the general shape of base 2 at 95% similarity and the rest 5% from base 1, with boundary of WM and GM from the average of all the five bases, voxel intensity of WM from base 4, voxel intensity of GM from base 1 at 30% and 70% from base 5, and ventricles from base 5 only. We may see that the brains generated appear

extremely realistic. We tested identification of the authenticity of these brains generated by using several brain anatomists who were blind to this study. None of them can correctly tell the artificial ones from the real ones, and some of them believed that all the images were real-world imaging data.

In the second experiment, we added one feature, cortical thickness, to this model. Based on our past studies in method development (Bansal et al., 2007) and those studying cortical thickness changes in healthy individuals (Sowell et al., 2007), children of Tourette's syndrome (Sowell et al., 2008), attention deficit/hyperactivity disorder (ADHD) (Bansal et al., 2007), high-risk familial depression (Peterson et al., 2009; Dubin et al., 2012), and chronic neuropsychiatric illness (Bansal et al., 2012), we simulated individual cortical thickness profiles for the five base brains, and tested deducing results based on them under various conditions. Traditional statistical analysis for studying cortical thickness will provide only one final set of results under a given condition, for example, the statistical pattern of group average. In contrast, our model can provide dynamic views of the results, freely and selectively use parts of the samples that are of interest for intuitive examination of possible results, and thus evaluate the difference among different subsets of the population (Fig. 4).

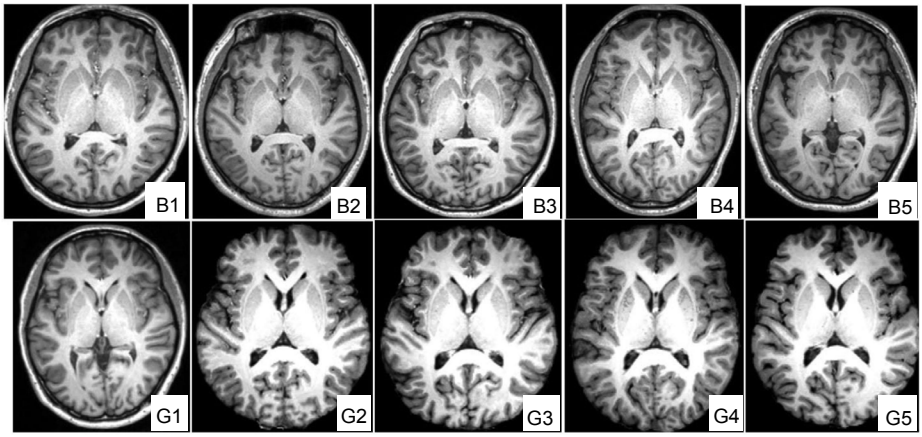

Fig. 3 Preliminary examples of generating realistic new brains using MSAG

The current generation involves only shape and intensity to demonstrate the feasibility of our design. The first row shows five different base brains, and the second row shows the generated brains, either with or without scalp, which look very realistic. The new brains vary in size, shape, and structures, as they blend features from the base brains with different weights. For example, G1 used the shapes of B1 and B2, but adopted different combinations of weights of structures and voxel intensities from all the five base brains; G2–G5 are additional instances of using various weights. Adding more variables such as imaging parameters will allow more delicate and complex controls over the results, and will generate more drastically different results

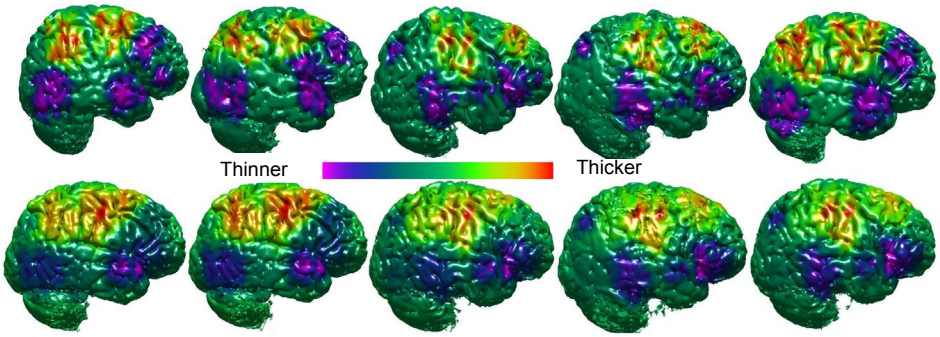

Fig. 4 Deducing cortical thickness

The upper row shows the pattern of the five base brains, and the bottom row shows several simulations based on the base brains using different control settings

For example, we can selectively see the statistical pattern from individuals 1, 3, and 5 of the same age (e.g., 32), or inspect the pattern of female, black subjects who hold a bachelor's degree, by conducting MSAG based on only subjects who hold these attributes. When the system has an adequate number of samples as the base brains, this work can be used to check dynamically the possible evolution course of the pattern from one age to the other, and simultaneously from healthy to diseased people that are hybrid of more than one race, although possibly none of the base brains was actually of more than one race. Similarly, our model can artificially deduce a prescribed virtual brain, for example, defined as female, aged 35.5, genetically 5-HTTLPR_rs25531AA who is developing post-stroke depression (Mak et al., 2013). The model can thus help investigators actually visualize and examine various possibilities, while no such person actually exists in the real world.

In the third experiment, we deduced MR images in different imaging conditions. The full details of this piece of work have been reported separately elsewhere (Jiang et al., 2017). In this experiment, we first acquired MRI data Img_1 under one imaging setting defined by a set of imaging parameters Set_1. We then used knowledge of physical properties (in particular, the T1/T2-relaxation times) that we have collected from standard samples of the base brains, and used them to deduce, for each voxel in Img_1, a new value in a virtual image Img_2 that is supposed to be collected under a different imaging setting defined by another set of imaging parameters Set_2. We also collected the actual dataset Img_{2a} in reality from the same person using the parameters defined by Set_2. We then compared Img_2 with Img_{2a} to inspect the effectiveness of our method (Fig. 5). The results showed that the deduction was successful, and that the deduced results were highly correlated with the actual scan (Fig. 6).

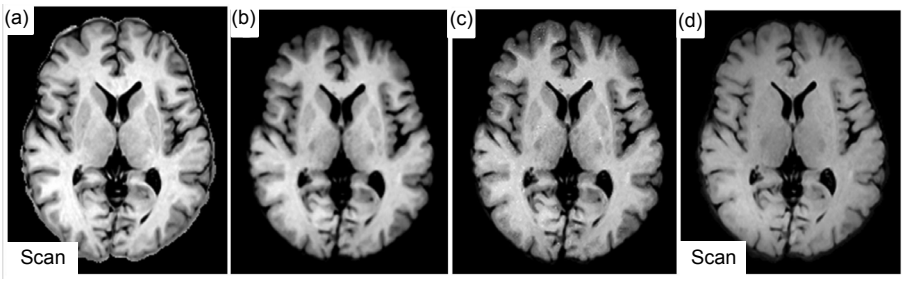

Fig. 5 Deducing T1w data using knowledge extracted from only four sample brains

(a) An actual scan Img_{2a} of subject J using imaging setting Set_2 (TR/TE/TI=9000/10/900 ms). (b) and (c) are J's artificially deduced images Img_2 at the same imaging setting of Set_2: (b) was smoothed with a 1-voxel (0.72 mm) kernel, and (c) was not smoothed. (d) is the actual scan acquired under imaging setting Set_1 (TR/TE/TI=9000/10/1500 ms), which was the initial image from which (b) and (c) were deduced. It can be seen that the deduced versions (b) and (c) are almost identical to (a)

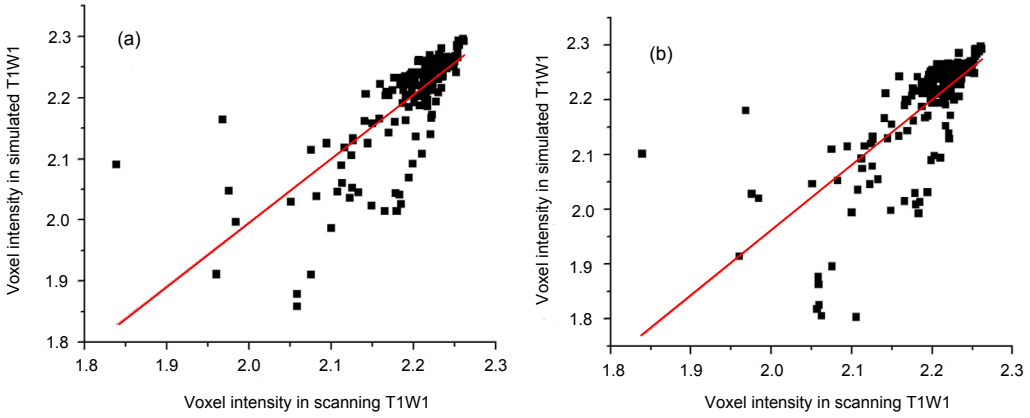

Fig. 6 Correlation *r* between the scanned and deduced data

(a) Figs. 5a and 5c: r=0.7544, y=−87.765+1.04x; if background voxels are included, r=0.9943, y=−3.264+1.00x. (b) Figs. 5a and 5b: r=0.7371, y=−428.75+1.20x; if background included, r=0.9967, y=−1.945+1.00x. Both are highly linearly correlated and matched, with minimum intercepts. The data shown here contained 218 voxels randomly picked from one image slice

4 Conclusions and discussion

We proposed an AI platform of digital brain for brain research, which can use crowd wisdom to integrate various types of knowledge on the brain. We first introduced the theory behind the design, then illustrated the idea and a blueprint, and finally demonstrated our preliminary progress. The first two examples showed how the platform will work based on sample datasets—the base brains span a reasoning space, and each point in the space is potentially a virtual and new human brain to be generated, defined by the variables along each feature axis in the reasoning space. At each such point, which corresponds to a virtual brain, the third example actually expanded it to a second level of detail, in which all the imaging parameters constitute another reasoning universe for reasoning new MRI data for this particular virtual brain. By setting the values of a number of different imaging parameters, the proposed work may generate imaging data under different imaging conditions, as if the same virtual person were scanned multiple times on a real scanner using different imaging settings.

Using the small universe thus expanded by the third experiment, we demonstrated the complexity of our proposed platform, which may nest different levels of a reasoning universe. Within only this small reasoning universe, a duplication of our proposed method of computational intelligence may also develop advanced and unique abilities: (1) It provides a function comparable to the software tool of Adobe Photoshop to fix MRI data, certainly, following the principles of MR imaging and MRI physics but not optics. This is useful if a patient was scanned using a set of imaging parameters that were not individually optimized and, therefore, the image contrast of the acquired data was not optimal. (2) It also provides a virtual software MR scanner, and a whole set of imaging data can be prescribed and then generated without going to an actual scanner, which is usually expensive in both time and money. As the method may deduce the physical property of the tissue at each voxel using prior knowledge that has been built using the base brains, the virtual scanner may generate data of other imaging modalities. For example, in the current case, as we have knowledge of T1/T2 relaxation times for various tissues collected from base brains, T1w data can be used to deduce T2w data, which typically can be acquired only by physically scanning real human subjects using a real MRI scanner.

The proposed platform is actually a digital brain database. Feeding into the system brain data including all associated data, such as imaging data, genetic data, demographic data, and EEG data, it automatically becomes a brain library. Setting values of interest to the feature variables that span the reasoning space, various information regarding human brains may be retrieved and automatically calculated. For example, input age=30–39, race=Asian, disease=schizophrenia, and sex=male; all brain data meeting these requirements will be presented. Moreover, if we set the weights equally to all the retrieved datasets, the MSAG framework will automatically generate an average brain image based on all the retrieved datasets, providing a statistical atlas of all Asian male schizophrenia patients in their 30s.

The proposed platform is also a digital brain phantom. Based on the computational AI model of MSAG/SR, the platform can use a limited number of sample base brains to deduce numerous new brains, just as parents may give birth to as many newborns (if age is not an issue). The features extracted from the brains span the reasoning space. The more the features, the higher the dimensionality of the reasoning space, and the more powerful the platform is in deducing new imaging data (phantoms). The deduced image can be very useful for testing new methodologies because affecting variables can now be fully controlled. Thus, the effectiveness of new image analytic methods can be well validated.

The platform is open in its nature, as its kernel, the computational MSAR method, is scalable. New axes that define new features can be added any time into the reasoning space, and new brain datasets can also be added any time to expand the bases for reasoning (just like more parents join to provide genes). Also, the more the brains representing different populations are added, the more powerful the platform is. For example, if the data contain brains of all ages of healthy people and also those with different diseases, the system will allow deducing either brain development of normal healthy people, or brain evolution from the healthy to the diseased, or vice versa. In particular, it can deduce brains of mixed disease conditions, which may be possibly not available in

reality. This gives scientists an ability to predict possibilities of certain diseases in the future, and they do not have to wait until such things actually happen 20 years later. The deduced results may not be exactly true, but the bottom line is that it provides something tangible that the scientists may play with and study. As another example, to communicate with colleagues or explain to a patient the possible route of disease evolution, a physician may prescribe the five-year-later version of a current diseased brain. The physician may present it now visually and vividly, instead of orally describing the situation, to a patient or a colleague, which may very possibly be misunderstood because the audience could imagine something that is totally different from what is orally described, due to variations or degree of the required professional knowledge.

The platform is indeed a knowledge system for brain and neuroscience. If many brain studies use the system, and all findings are fed into the system, the platform will be able to merge knowledge, and to solve conflicts in findings if findings from similar studies disagree with or contradict each other. For example, one study may find major depressive disorder (MDD) leads to a smaller hippocampus, whereas the other may have found that the hippocampus of MDD statistically becomes larger. With data from both sides available in the same platform, the system may now examine where such conflicts come from and thereby solve them by a joint and cross analysis.

The current report presented our preliminary progress in this project. In this work, we used only five subject brains to demonstrate the feasibility of the proposed idea. The next step is to expand the number of samples, making it more powerful. Obviously, the size of the sample data and the number of users are important factors to the success of this platform. Big data will provide a comprehensive coverage to support all the feature axes with adequate samples, which are the source of the needed knowledge to run the system. It also forms the basis on which potential users may thereby make effective inquiries, consequently allowing the system to deduce new data prescribed by the users. On the other hand, intensive use of the system from various users across different disciplines is desirable, as this will provide crowd wisdom to the system. A large number of users will provide feedbacks of new findings associated with the brain data in the system, and their behaviors in using the system will thereby provide new domain knowledge and information on linking the data entities in the system. The latter basically forms the edges in a knowledge graph, which will enhance the reasoning and deducing abilities of our platform. To attract more users to use the system, a set of software tools for analyzing neuroimaging data is needed, so that data and findings can be uniformly processed using the same data interfaces and formats, and subsequently the related data can be easily employed in the system to implement the goals as discussed earlier. The tools can use those we have developed in-house (Xu et al., 2003, 2008; Plessen et al., 2006; Liu F et al., 2006, 2008, 2010; Liu W et al., 2012a, b; Bansal et al., 2013; Hao et al., 2013; Liu X et al., 2013; Wen et al., 2013), or those freely available online, such as SPM12, FSL, and FreeSurfer. However, using the latter would need a set of interfaces for converting the data formats for mutual-compatibility.

Acknowledgements

Special thanks to Professor Yunhe Pan for the inspiring meeting and discussion in 2014, which initialized this work.

References

Amunts K, Schleicher A, Bürgel U, et al., 1999. Broca's region revisited: cytoarchitecture and intersubject variability. *J Comp Neurol*, 412(2):319-341. https://doi.org/10.1002/(SICI)1096-9861(19990920)412:2<319::AID-CNE10>3.0.CO;2-7

Arnold JB, Liow JS, Schaper KA, et al., 2001. Qualitative and quantitative evaluation of six algorithms for correcting intensity nonuniformity effects. *NeuroImage*, 13(5):931-943. https://doi.org/10.1006/nimg.2001.0756

Aubert-Broche B, Evans AC, Collins L, 2006. A new improved version of the realistic digital brain phantom. *NeuroImage*, 32(1):138-145. https://doi.org/10.1016/j.neuroimage.2006.03.052

Baars BJ, Gage NM, 2010. Cognition, Brain, and Consciousness: Introduction to Cognitive Neuroscience (2nd Ed.). Elsevier, p.591-616. https://doi.org/10.1016/B978-0-12-375070-9.00021-8

Bansal R, Xu D, Peterson BS, 2005. Eigen function based coregistration of diffusion tensor images to anatomical magnetic resonance images. *Proc Int Soc Magn Reson Med*, 13:2332.

Bansal R, Staib LH, Xu DR, et al., 2007. Statistical analyses of brain surfaces using gaussian random fields on 2-D manifolds. *IEEE Trans Med Imag*, 26(1):46-57. https://doi.org/10.1109/TMI.2006.884187

Bansal R, Staib LH, Laine AF, et al., 2012. Anatomical brain images alone can accurately diagnose chronic neuropsy-

chiatric illnesses. *PloS ONE*, 7(12):e50698. https://doi.org/10.1371/journal.pone.0050698

Bansal R, Hao XJ, Liu F, et al., 2013. The effects of changing water content, relaxation times, and tissue contrast on tissue segmentation and measures of cortical anatomy in MR images. *Magn Reson Imag*, 31(10):1709-1730. https://doi.org/10.1016/j.mri.2013.07.017

Bastin ME, 1999. Correction of eddy current-induced artefacts in diffusion tensor imaging using iterative cross-correlation. *Magn Reson Imag*, 17(7):1011-1024. https://doi.org/10.1016/S0730-725X(99)00026-0

Bastin ME, 2001. On the use of the FLAIR technique to improve the correction of eddy current induced artefacts in MR diffusion tensor imaging. *Magn Reson Imag*, 19(7): 937-950. https://doi.org/10.1016/S0730-725X(01)00427-1

Bastin ME, Armitage PA, 2000. On the use of water phantom images to calibrate and correct eddy current induced artefacts in MR diffusion tensor imaging. *Magn Reson Imag*, 18(6):681-687. https://doi.org/10.1016/S0730-725X(00)00158-2

Belliveau JW, Kennedy DNJr, McKinstry RC, et al., 1991. Functional mapping of the human visual cortex by magnetic resonance imaging. *Science*, 254(5032):716-719. https://doi.org/10.1126/science.1948051

Bohland JW, Bokil H, Allen CB, et al., 2009. The brain atlas concordance problem: quantitative comparison of anatomical parcellations. *PLoS ONE*, 4(9):e7200. https://doi.org/10.1371/journal.pone.0007200

Bradley MM, Sabatinelli D, Lang PJ, et al., 2003. Activation of the visual cortex in motivated attention. *Behav Neurosci*, 117(2):369-380. https://doi.org/10.1037/0735-7044.117.2.369

Brown RW, Cheng YCN, Haacke EM, et al., 2014. Magnetic Resonance Imaging: Physical Principles and Sequence Design (2nd Ed.). Wiley Blackwell, New York. https://doi.org/10.1002/9781118633953

Davatzikos C, 1996a. Nonlinear registration of brain images using deformable models. Proc Workshop on Mathematical Methods in Biomedical Image Analysis, p.94-103. https://doi.org/10.1109/MMBIA.1996.534061

Davatzikos C, 1996b. Spatial normalization of 3D brain images using deformable models. *J Comput Assist Tomogr*, 20(4):656-665. https://doi.org/10.1097/00004728-199607000-00031

Davatzikos C, 1997. Spatial transformation and registration of brain images using elastically deformable models. *Comput Vis Image Underst*, 66(2):207-222. https://doi.org/10.1006/cviu.1997.0605

Davatzikos C, Genc A, Xu DR, et al., 2001. Voxel-based morphometry using the RAVENS maps: methods and validation using simulated longitudinal atrophy. *NeuroImage*, 14(6):1361-1369. https://doi.org/10.1006/nimg.2001.0937

DeYoe EA, Carman GJ, Bandettini P, et al., 1996. Mapping striate and extrastriate visual areas in human cerebral cortex. *PNAS*, 93(6):2382-2386. https://doi.org/10.1073/pnas.93.6.2382

Dubin M, Weissman M, Xu DR, et al., 2012. Identification of a circuit-based endophenotype for familial depression. *Psych Res Neuroimag*, 201(3):175-181. https://doi.org/10.1016/j.pscychresns.2011.11.007

Evans AC, 2006. The NIH MRI study of normal brain development. *NeuroImage*, 30(1):184-202. https://doi.org/10.1016/j.neuroimage.2005.09.068

Fagiolo G, Waldman A, Hajnal JV, 2008. A simple procedure to improve FMRIb software library brain extraction tool performance. *Br J Radiol*, 81(963):250-251. https://doi.org/10.1259/bjr/12956156

Fan LY, 2013. Development of Artifact-Free Imaging System and fMRI Research Paradigm for Creative Thinking in an MR-Compatible Environment. MS Thesis, East China Normal University, Shanghai, China (in Chinese).

Fan LY, Fan XF, Luo WC, et al., 2014. An explorative fMRI study of human creative thinking using: a specially designed iCAD system. *Acta Psychol Sin*, 46(4):427-436 (in Chinese). https://doi.org/10.3724/SP.J.1041.2014.00427

Hagmann P, Cammoun L, Gigandet X, et al., 2010. MR connectomics: principles and challenges. *J Neurosci Methods*, 194(1):34-45. https://doi.org/10.1016/j.jneumeth.2010.01.014

Hagoort P, 2005. On broca, brain, and binding: a new framework. *Trends Cogn Sci*, 9(9):416-423. https://doi.org/10.1016/j.tics.2005.07.004

Hao XJ, Xu DR, Bansal R, et al., 2013. Multimodal magnetic resonance imaging: the coordinated use of multiple, mutually informative probes to understand brain structure and function. *Human Brain Map*, 34(2):253-271. https://doi.org/10.1002/hbm.21440

Haselgrove JC, Moore JR, 1996. Correction for distortion of echo-planar images used to calculate the apparent diffusion coefficient. *Magn Reson Med*, 36(6):960-964. https://doi.org/10.1002/mrm.1910360620

Hsu JL, Leemans A, Bai CH, et al., 2008. Gender differences and age-related white matter changes of the human brain: a diffusion tensor imaging study. *NeuroImage*, 39(2):566-577. https://doi.org/10.1016/j.neuroimage.2007.09.017

Huster RJ, Westerhausen R, Kreuder F, et al., 2009. Hemispheric and gender related differences in the Midcingulum bundle: a DTI study. *Human Brain Map*, 30(2):383-391. https://doi.org/10.1002/hbm.20509

Jack CRJr, Bernstein MA, Fox NC, et al., 2008. The Alzheimer's disease neuroimaging initiative (ADNI): MRI methods. *J Magn Reson Imag*, 27(4):685-691. https://doi.org/10.1002/jmri.21049

Jiang YW, Liu F, Fan MX, et al., 2017. Deducing magnetic resonance neuroimages based on knowledge from samples. *Comput Med Imag Graph*, 62:1-14. https://doi.org/10.1016/j.compmedimag.2017.07.005

Kanungo T, Mount DM, Netanyahu NS, et al., 2002. An efficient k-means clustering algorithm: analysis and implementation. *IEEE Trans Patt Anal Mach Intell*, 24(7):881-892. https://doi.org/10.1109/TPAMI.2002.1017616

Liu F, Peterson B, Duan Y, et al., 2006. Fast spin echo for T2

quantification at 3T. Proc 14th Scientific Meeting of the International Society for Magnetic Resonance in Medicine, p.2404.

Liu F, Garland M, Duan YS, et al., 2008. Study of the development of fetal baboon brain using magnetic resonance imaging at 3 Tesla. *NeuroImage*, 40(1):148-159. https://doi.org/10.1016/j.neuroimage.2007.11.021

Liu F, Garland M, Duan YS, et al., 2010. Techniques for *in utero*, longitudinal MRI of fetal brain development in baboons at 3 T. *Methods*, 50(3):147-156. https://doi.org/10.1016/j.ymeth.2009.03.019

Liu W, Liu XZ, Yang G, et al., 2012a. Improving the correction of eddy current-induced distortion in diffusion-weighted images by excluding signals from the cerebral spinal fluid. *Comput Med Imag Graph*, 36(7):542-551. https://doi.org/10.1016/j.compmedimag.2012.06.004

Liu W, Liu XZ, He XF, et al., 2012b. Spatial normalization of diffusion tensor images with voxel-wise reconstruction of the diffusion gradient direction. Proc 2nd Int Conf on Multimodal Brain Image Analysis, p.134-146. https://doi.org/10.1007/978-3-642-33530-3_11

Liu XZ, Yuan ZM, Zhu JM, et al., 2013. Medical image registration by combining global and local information: a chain-type diffeomorphic demons algorithm. *Phys Med Biol*, 58(23):8359-8378. https://doi.org/10.1088/0031-9155/58/23/8359

Lorenzi M, Ayache N, Frisoni G, et al., 2010. 4D registration of serial brain's MR images: a robust measure of changes applied to Alzheimer's disease. Miccai Workshop on Spatio-Temporal Image Analysis for Longitudinal and Time-Series Image Data.

Lynch G, 1979. Representations in the brain. *Science*, 204(4394):762. https://doi.org/10.1126/science.204.4394.762

Maguire EA, 2001. Neuroimaging, memory and the human hippocampus. *Rev Neurol*, 157(8-9 Pt 1):791-794.

Mak KK, Kong WY, Mak A, et al., 2013. Polymorphisms of the serotonin transporter gene and post-stroke depression: a meta-analysis. *J Neurol Neurosurg Psych*, 84(3):322-328. https://doi.org/10.1136/jnnp-2012-303791

Michelucci P, Dickinson JL, 2016. The power of crowds. *Science*, 351(6268):32-33. https://doi.org/10.1126/science.aad6499

Neeb H, Zilles K, Shah NJ, 2006. Fully-automated detection of cerebral water content changes: study of age- and gender-related H_2O patterns with quantitative MRI. *NeuroImage*, 29(3):910-922. https://doi.org/10.1016/j.neuroimage.2005.08.062

Ng HP, Ong SH, Foong KWC, et al., 2006. Medical image segmentation using *k*-means clustering and improved Watershed algorithm. IEEE Southwest Symp on Image Analysis and Interpretation, p.61-65. https://doi.org/10.1109/SSIAI.2006.1633722

Nickel M, Murphy K, Tresp V, et al., 2016. A review of relational machine learning for knowledge graphs. *Proc IEEE*, 104(1):11-33. https://doi.org/10.1109/JPROC.2015.2483592

Packard MG, White NM, 1991. Dissociation of hippocampus and caudate nucleus memory systems by posttraining intracerebral injection of dopamine agonists. *Behav Neurosci*, 105(2):295-306. https://doi.org/10.1037/0735-7044.105.2.295

Pan YH, 1996. The synthesis reasoning. *Patt Recogn Artif Intell*, 9(3):201-208 (in Chinese).

Pan YH, 1997. Intelligent CAD Methodology and Modeling. Science Press, Beijing, China (in Chinese).

Peterson BS, Warnera V, Bansal R, et al., 2009. Cortical thinning in persons at increased familial risk for major depression. *PNAS*, 106(15):6273-6278. https://doi.org/10.1073/pnas.0805311106

Plessen KJ, Grüner R, Lundervold A, et al., 2006. Reduced white matter connectivity in the corpus callosum of children with Tourette syndrome. *J Child Psychol Psych*, 47(10):1013-1022. https://doi.org/10.1111/j.1469-7610.2006.01639.x

Rhodes G, Brennan S, Carey S, 1987. Identification and ratings of caricatures: implications for mental representations of faces. *Cogn Psychol*, 19(4):473-497. https://doi.org/10.1016/0010-0285(87)90016-8

Schreibmann E, Thorndyke B, Li TF, et al., 2008. Four-dimensional image registration for image-guided radiotherapy. *Int J Radiat Oncol Biol Phys*, 71(2):578-586. https://doi.org/10.1016/j.ijrobp.2008.01.042

Shapiro ML, Eichenbaum H, 1999. Hippocampus as a memory map: Synaptic plasticity and memory encoding by hippocampal neurons. *Hippocampus*, 9(4):365-384. https://doi.org/10.1002/(SICI)1098-1063(1999)9:4<365::AID-HIPO4>3.0.CO;2-T

Shen DG, Davatzikos C, 2002. HAMMER: hierarchical attribute matching mechanism for elastic registration. *IEEE Trans Med Imag*, 21(11):1421-1439. https://doi.org/10.1109/TMI.2002.803111

Shen DG, Davatzikos C, 2003. Very high-resolution morphometry using mass-preserving deformations and HAMMER elastic registration. *NeuroImage*, 18(1):28-41. https://doi.org/10.1006/nimg.2002.1301

Shen DG, Davatzikos C, 2004. Measuring temporal morphological changes robustly in brain MR images via 4-dimensional template warping. *NeuroImage*, 21(4):1508-1517. https://doi.org/10.1016/j.neuroimage.2003.12.015

Shen DG, Sundar H, Xue Z, et al., 2005. Consistent estimation of cardiac motions by 4D image registration. *LNCS*, 3750: 902-910. https://doi.org/10.1007/11566489_111

Sowell ER, Peterson BS, Kan E, et al., 2007. Sex differences in cortical thickness mapped in 176 healthy individuals between 7 and 87 years of age. *Cerebr Cort*, 17(7):1550-1560. https://doi.org/10.1093/cercor/bhl066

Sowell ER, Kan E, Yoshii J, et al., 2008. Thinning of sensorimotor cortices in children with tourette syndrome. *Nat Neurosci*, 11(6):637-639. https://doi.org/10.1038/nn.2121

Sporns O, 2011. The human connectome: a complex network. *Ann New York Acad Sci*, 1224(1):109-125. https://doi.org/10.1111/j.1749-6632.2010.05888.x

Squire LR, 1992. Memory and the hippocampus: a synthesis from findings with rats, monkeys, and humans. *Psychol Rev*, 99(2):195-231.

Toga AW, Clark KA, Thompson PM, et al., 2012. Mapping the human connectome. *Neurosurgery*, 71(1):1-5. https://doi.org/10.1227/NEU.0b013e318258e9ff

van Essen DC, Smith SM, Barch DM, et al., 2013. The WU-Minn Human Connectome Project: an overview. *NeuroImage*, 80:62-79. https://doi.org/10.1016/j.neuroimage.2013.05.041

van Hecke W, Sijbers J, de Backer S, et al., 2009. On the construction of a ground truth framework for evaluating voxel-based diffusion tensor MRI analysis methods. *NeuroImage*, 46(3):692-707. https://doi.org/10.1016/j.neuroimage.2009.02.032

Wen Y, Peterson BS, Xu DR, 2013. A highly accurate, optical flow-based algorithm for nonlinear spatial normalization of diffusion tensor images. Int Joint Conf on Neural Networks, p.1-8. https://doi.org/10.1109/IJCNN.2013.6706989

Xu DR, 1995. A Study of Analogical Generation of Image in Designing, in Computer Science. PhD Thesis, Zhejiang University, Hangzhou, China, p.120 (in Chinese).

Xu DR, 1998. Automated analogical design of newspaper page layout. *Chin J Comput*, 21(12):1066-1073 (in Chinese). https://doi.org/10.3321/j.issn:0254-4164.1998.12.002

Xu DR, Pan YH, 1995. Generation-oriented analogy reasoning. *Sci China*, 38(9):150-167

Xu DR, Mori S, Shen DG, et al., 2003. Spatial normalization of diffusion tensor fields. *Magn Reson Med*, 50(1):175-182. https://doi.org/10.1002/mrm.10489

Xu DR, Hao XJ, Bansal R, et al., 2008. Seamless warping of diffusion tensor fields. *IEEE Trans Med Imag*, 27(3):285-299. https://doi.org/10.1109/TMI.2007.901428

Zhuang JC, Hrabe J, Kangarlu A, et al., 2006. Correction of eddy-current distortions in diffusion tensor images using the known directions and strengths of diffusion gradients. *J Magn Reson Imag*, 24(5):1188-1193. https://doi.org/10.1002/jmri.20727